Check for updates

ANTHROPOLOGY

The phylogenetic position of the Yunxian cranium elucidates the origin of *Homo longi* and the Denisovans

Xiaobo Feng[1,2,3,4]†, Qiyu Yin[5,6]†, Feng Gao[7]†, Dan Lu[5,6]†, Qin Fang[8], Yilu Feng[9], Xuchu Huang[10], Chen Tan[11], Hanwen Zhou[12], Qiang Li[5,6], Chi Zhang[5,6], Chris Stringer[13]*, Xijun Ni[5,6,14]*

Diverse forms of *Homo* coexisted during the Middle Pleistocene. Whether these fossil humans represent different species or clades is debated. The ~1-million-year-old Yunxian 2 fossil from China is important for understanding the cladogenesis of *Homo* and the origin of *Homo sapiens*. In this study, we restored and reconstructed the distorted Yunxian 2 cranium using recently introduced technology. The results show that this cranium displays mosaic primitive and derived features. Morphometric and phylogenetic analyses suggest that it is an early member of the Asian *H. longi* clade, which includes the Denisovans and is the main part of the sister group to the *H. sapiens* clade. Both the *H. sapiens* and *H. longi* clades have deep roots extending beyond the Middle Pleistocene and probably experienced rapid early diversification. Yunxian 2 may preserve transitional features close to the origins of the two clades.

Middle Pleistocene (Chibanian) human fossils show high morphological diversity. Some of the fossils discovered recently, such as those from Callao Cave in the Philippines, Rising Star Cave in South Africa, and Harbin in China, are so different from other fossil humans that they have been proposed as new species (*1*–*3*), distinct from previously identified taxa such as *Homo sapiens*, *H. neanderthalensis*, *H. heidelbergensis*, *H. erectus*, and *H. habilis*. It remains a matter of intense debate whether these morphologically diverse archaic humans represent multiple evolutionary clades or whether they are transitional variants leading to *H. sapiens*. Chibanian human fossils from China, sometimes called "archaic *Homo sapiens*," have been at the center of fierce debates about their relationship to *H. sapiens* for many years. Because of their even greater antiquity (*4*, *5*) and apparent possession of both primitive features of *H. erectus* and, arguably, derived features of *H. sapiens* (*6*, *7*), the two fossil crania—Yunxian 1 and 2—from a site on a terrace of the Hanjiang River in the Yunyang district (formerly Yunxian City) of Shiyan City, Hubei Province, China, are important for interpreting the Chibanian record in China and reconstructing the evolution of *Homo* more generally. The better preserved of the two crania, Yunxian 2, is nevertheless distorted, which has hampered attempts to infer its phylogenetic position. We reconstructed Yunxian 2, also incorporating elements from Yunxian 1, and investigated its phylogenetic position. Given its geological age of 0.94 to 1.10 million years (Ma) (*5*) and the presence of mosaic primitive and derived features, we argue that Yunxian 2 probably lies close to the last common ancestor of the clades containing *H. sapiens* and *H. longi* (hereafter called the sapiens clade and longi clade, respectively) and can also elucidate the evolutionary history of the Denisovans.

Our understanding of human evolution is largely based on fossil cranial specimens, but many of these are incompletely preserved and/or distorted. Proper reconstruction of these imperfect fossils is therefore critical to studying their phylogenetic relationships. Reconstructions of material such as *Sahelanthropus*, *Ardipithecus*, *Paranthropus*, *H. habilis*, and the Chibanian Steinheim and Ceprano *Homo* crania have already provided essential evidence regarding the early stages of human evolution (*8*–*15*).

The Yunxian human fossil site has yielded three crania so far [including the recently discovered and still unprepared Yunxian 3 (*16*)]. Two previously known Yunxian crania, Yunxian 1 and 2, are both distorted. Yunxian 1 is crushed, with obvious plastic deformation, whereas the distortion of Yunxian 2 is much less severe. Evaluation of high-resolution computed tomography (CT) scans indicates that the primary distortion is due to fragmentation and displacement rather than plastic deformation, which involves twisting, banding, or flattening of a curved surface when subjected to continuous force or stress [see supplementary materials (SM)]. In a previous study, this cranium was virtually reconstructed primarily through landmark-based realignment and mirroring of the counterpart (*17*). The new reconstruction reported here is based on the least distorted cranium, Yunxian 2, but also uses some data from Yunxian 1. The CT scans showed that the distortion of Yunxian 2 consisted mainly of small fractures and displacement of large fragments. We used methods that were developed in recent years (*8*–*13*), including CT image segmentation (digitally splitting the fossil bones from the matrix) and separation and repositioning of the fragments, to correct the distortion (see SM for the detailed reconstruction procedure and evaluation of the different reconstruction versions).

Mosaic morphology

As reconstructed, the Yunxian 2 cranium is large and long, with a broad and flat (platycephalic) braincase in lateral view (Fig. 1). It is smaller than the Harbin cranium (*H. longi*) and Xuchang; about the same size as Kabwe, Petralona, Bodo, Jinniushan, and Sangiran 17; and larger than the Jebel Irhoud 1, Dali, and Maba specimens in overall dimensions. After reconstruction, the fossil lacks only small parts of the zygomatic arches and the missing central incisors. The cranium is clearly plesiomorphic in overall form, presenting primitive traits shared by earlier hominins, such as a thick supraorbital torus, a broad basicranium and palate, a long and low vault in lateral view, a receding frontal contour, and a rather flat parietal contour. However, it lacks both the strongly angulated occipital with a prominent transverse torus found in *H. erectus* and some Chibanian African and European *Homo* crania as well as the protruding occipital region (occipital bun) with a central suprainiac fossa typical of Neanderthals. In posterior view (Fig. 1B), the slightly keeled cranium is widest in the supramastoid region, below which the large mastoid processes slope inward. Additionally, the temporals and parietals converge superiorly, although not as strongly as in *H. erectus* fossils, and there is neither the upper parietal expansion found in recent *H. sapiens* nor the "en bombe" shape typical of Neanderthals. In lateral view (Fig. 1, E and F), the face is high and projects anteriorly as in *H. erectus* and Chibanian African and European *Homo* fossils, but to a smaller degree. The nasal bones also project strongly anteriorly, but the midface is not pulled forward as in Neanderthals. The upper face and nasal aperture are wide. The zygomaxillary region is transversely flat and faces anteriorly, more comparable to the condition in European *H. antecessor* and the Asian Harbin, Dali, Jinniushan,

[1]School of History and Culture, Shanxi University, Taiyuan, China. [2]Hubei Polytechnic University, Huangshi, China. [3]Institute of Yunxian Man Site, Hanjiang Normal University, Shiyan, China. [4]School of History, Culture and Tourism, Hanjiang Normal University, Shiyan, China. [5]Institute of Vertebrate Paleontology and Paleoanthropology, Chinese Academy of Sciences, Beijing, China. [6]College of Earth and Planetary Sciences, University of Chinese Academy of Sciences, Beijing, China. [7]Yunnan Institute of Cultural Relics and Archaeology, Kunming, China. [8]Hubei Provincial Institute of Cultural Relics and Archaeology, Wuhan, China. [9]School of History of Wuhan University, Wuhan, China. [10]Museum of Shiyan, Shiyan, China. [11]Poly Art Research Institute, Beijing, China. [12]School of Earth Sciences, China University of Geosciences, Wuhan, China. [13]Centre for Human Evolution Research, Natural History Museum, London, UK. [14]PaleoAnthropological Research Center, Fudan University, Shanghai, China.
***Corresponding author. Email: nixijun@ivpp.ac.cn (X.N.); c.stringer@nhm.ac.uk (C.S.)**
†These authors contributed equally to this work.

Downloaded from https://www.science.org at Tsinghua University on September 26, 2025



Fig. 1. Reconstruction of the Yunxian 2 cranium in standard views. (**A** to **F**) Anterior, posterior, inferior, superior, left, and right views, respectively. Brown color indicates the fossil bone. The zygomatic bone and the tip of the left maxilla, as indicated with dark brown, were grafted and reconstructed by incorporating elements of Yunxian 1. White color indicates the reconstructed parts inferred from the fracture edge and Yunxian 1. Neutral gray indicates the bones crushed and covered by other bones and matrix. Scale bar, 5 cm.

and Hualongdong fossils as well as in *H. sapiens*. However, the cheekbones are large and high.

The matrix enclosed in the endocranial cavity of Yunxian 2 is very dense, and the bone-matrix contrast of the CT scan is low. As a result, anatomical details such as the cranial vessel impressions on the inner surface of the cranial bones of Yunxian 2 cannot yet be reconstructed. Nevertheless, by setting 28 landmarks and measuring bone thickness, we were able to reconstruct the gross endocranial impressions (Fig. 2) and show that Yunxian 2 has a moderate endocranial capacity of about 1143 cm^3, similar to Dali, Hualongdong, Arago 21, Petralona, and Ceprano. Its frontal lobe is low and narrow, barely more expanded than those of *H. erectus* and Chibanian African and European *Homo* crania and considerably less expanded than those of Neanderthals [including the Sima de los Huesos fossils (*18*)] and *H. sapiens*. The posterior parts of the parietal and occipital lobes are laterally and posteriorly expanded to a degree similar to Kabwe, Petralona, Dali, Jinniushan, Xuchang, and Neanderthals. The dorsal expansion of the parietal lobe of Yunxian 2 is much less than that of Neanderthals and *H. sapiens*.

The Yunxian 2 cranium shows a distinctive combination of traits. It provides new anatomical details for systematic comparison, inferring phylogenetic position, and testing phylogenetic models for the genus *Homo* in general. Geometric morphometric analysis based on 533 landmarks and semilandmarks (see SM) shows that the 26 most complete hominin fossils and 153 recent human specimens compared with the reconstructed Yunxian 2 clustered into several groups in the morphospace of bgPCA 1 and bgPCA 2 (bgPCA, between-group principal components analysis) (Fig. 3). As the shape extremes indicate, lower bgPCA 1 values represent a more retracted and smaller face and a more globular neurocranium, whereas higher bgPCA 1 values represent a larger and more projecting face, a low and small neurocranium, a stronger supraorbital torus, and a stronger occipital torus. Lower bgPCA 2 values represent a narrower face and higher neurocranium, whereas higher bgPCA 2 values represent a broader and lower face, stronger supraorbital torus, lower but more elongated neurocranium, and more protruding occipital region. Dali, Jinniushan, Harbin, and Yunxian 2 all have moderate bgPCA 1 values but higher bgPCA 2 values, grouping them in a distinctive position. Along the bgPCA 1, Yunxian is within the range of *H. erectus*/*H. ergaster* and also close to Petralona. Neanderthals, Kabwe, Harbin, Dali, Jinniushan, and Jebel Irhoud 1 lie between *H. erectus*/*H. ergaster* and the Late Pleistocene and modern *H. sapiens* groups. Along the bgPCA 2, however, Yunxian is clearly higher than *H. sapiens*, *H. erectus*/*H. ergaster*, Neanderthals, Petralona, and Kabwe and close to Jinniushan. Overall, the position of Yunxian 2 in morphospace reflects its intermediate morphology between *H. erectus*/*H. ergaster*, Kabwe and Petralona, and the group including Harbin, Dali, and Jinniushan. When the phylogenetic relationship of Yunxian 2 is mapped onto the morphospace (Fig. 3, gray lines), Yunxian shows a close relationship with Harbin, Dali, and Jinniushan, which supports its grouping with them.

The longi clade

Phylogenetic analyses including Yunxian 2, using the parsimony criterion and Bayesian tip-dating to estimate the divergence dates, reveal similar phylogenetic relationships to previous results (*19*). To assess the robustness of the phylogenetic inferences based on our restoration and reconstruction of Yunxian 2, we used the bootstrap method to resample its character scoring (see details in the SM). The results suggest that potential errors in our restoration and reconstruction of

Downloaded from https://www.science.org at Tsinghua University on September 26, 2025

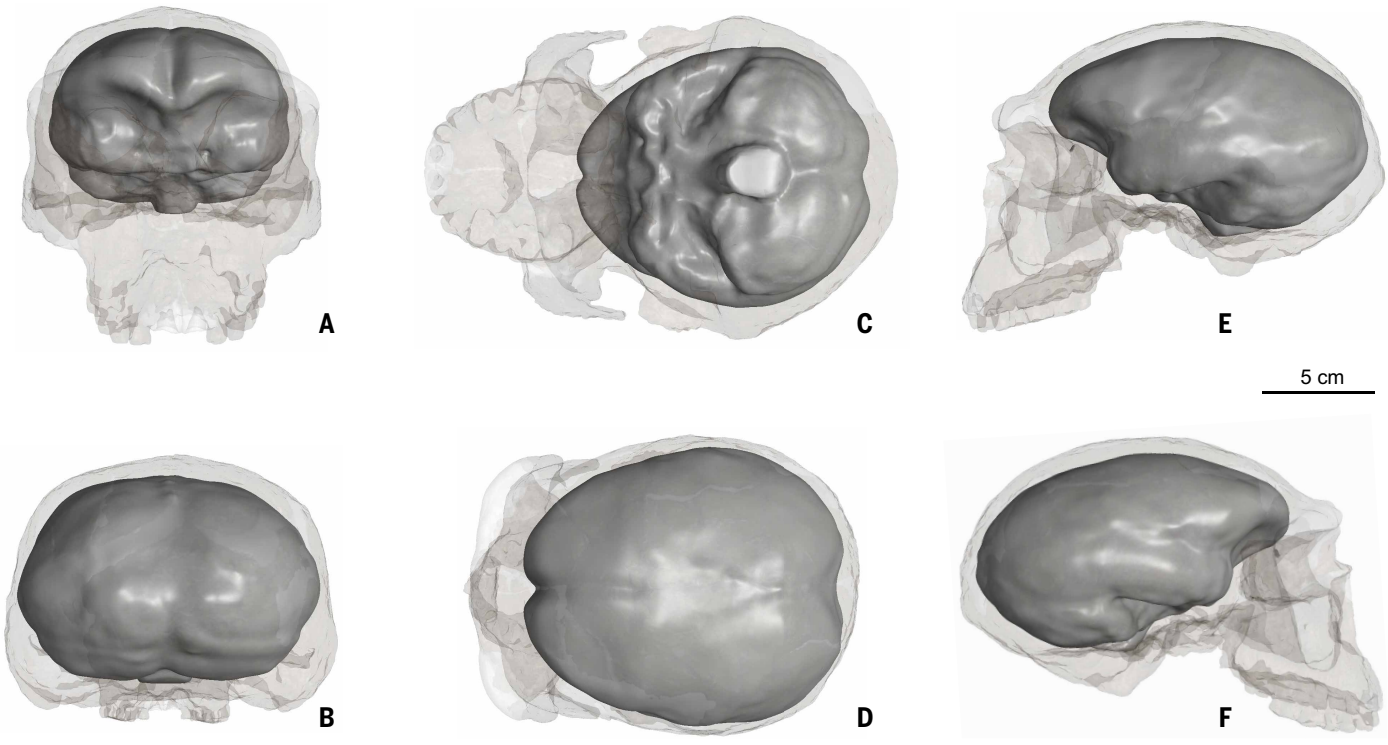


Fig. 2. Reconstruction of the endocranial cast of Yunxian 2. (**A** to **F**) Anterior, posterior, inferior, superior, left, and right views, respectively. Scale bar, 5 cm.

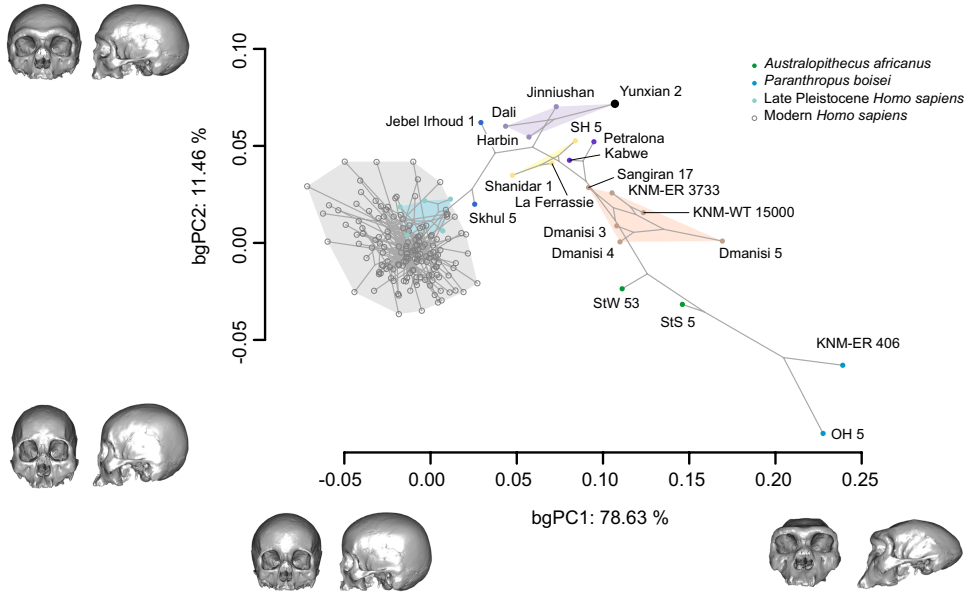


Fig. 3. Between-group principal components analysis of the Procrustes superimposed 533 landmarks and semilandmarks for 179 fossil and recent *Homo* specimens. The first two bgPCs are shown, with the reconstruction of Yunxian 2 projected onto the morphospace. The anterior and lateral views of the crania shown at the bottom and left of the bgPC axes represent the shape extremes of bgPC1 and bgPC2. These shape extremes were created on the basis of the mean shape (specimen YNO227) of all specimens analyzed (see supplementary materials for details). Gray lines show the phylogenetic relationships between fossil and recent *Homo* specimens, based on the phylogenetic analyses in this study. The relationship between recent specimens is a random tree and is based on the assumption that the recent population is monophyletic.

Yunxian 2 and in our discrete and metric character scoring have very little influence on the phylogenetic inferences we have made. The results of our phylogenetic analysis (Fig. 4) show that most Asian Chibanian hominins, previously often referred to as "archaic *Homo sapiens*," including Dali, Jinniushan, Xujiayao, and Hualongdong, are grouped together with the Xiahe and Penghu mandibles to form the monophyletic longi clade. This clade, plus *H. antecessor*, is the sister clade to the monophyletic sapiens clade. Recently, Xujiayao, Xuchang, Xiahe, Penghu, and Denisovans were proposed as a new species of *Homo* (*20*). Our phylogenetic analysis shows that these *Homo* samples (except for Xuchang) instead belong to the monophyletic longi clade. Yunxian has the greatest age within the longi clade, although it is not the most basal fossil in that clade from our results.

The Denisova Cave in the Altai Mountains has yielded fragmentary fossil humans that have been genetically identified as representing a clade distinct from *H. sapiens* and Neanderthals (*21*, *22*). Analyses of mitochondrial DNA place Denisovans with the Sima de los Huesos fossils and outside the divergence between *H. sapiens* and Neanderthals (*23*–*25*), whereas nuclear genome sequences suggest that Denisovans are a sister group to Neanderthals (*25*, *26*). With

Downloaded from https://www.science.org at Tsinghua University on September 26, 2025

only three clades (sapiens, Neanderthals, and Denisovans), both possible phylogenetic relationships, as reflected in the form of a tree topology (Fig. 4), are equally logical and depend on the choice of the rooting point of the tree; it is also possible that analyses of separately inherited mitochondrial and autosomal DNA will give different results. Our parsimony analysis, based on the limited number of informative characters scored for the Denisovans, suggests that Denisovans most likely belong to the longi clade.

The longi clade shared nine derived characters (synapomorphies) (table S5), such as larger cranial capacity, lower and longer frontal squama, narrower interorbital breadth, deeper glabellar inflexion, and so on. These characters are evident in the reconstructed morphology of Yunxian 2. The monophyly of the longi + *H. antecessor* + sapiens clade is also well supported. The synapomorphies of this larger group include 31 characters, such as narrower supraorbital torus breadth, narrower interorbital breadth, smaller palate, smaller malar height, presence of maxillary flexion, coronally oriented infraorbital plate, and a gracile phalanx without ungual tuberosity expansion. The Denisovans are known from very few specimens. Their derived features shared with other fossil humans of the longi clade and shown in the preserved specimens include reduction of the metacone of the upper M3, strengthening of the Carabelli's cusp of M2, reduction of the M2 width, increases in M2 hypocone and cusp 5 size, and development of an M3 crista obliqua. Morphological study of the Denisovan phalanx indicated that its dimensions and shape are within the range of *H. sapiens* (*27*). A gracile phalanx without expansion of the ungual tuberosity is also present in Jinniushan (*28*), a member of the longi clade in our analyses.

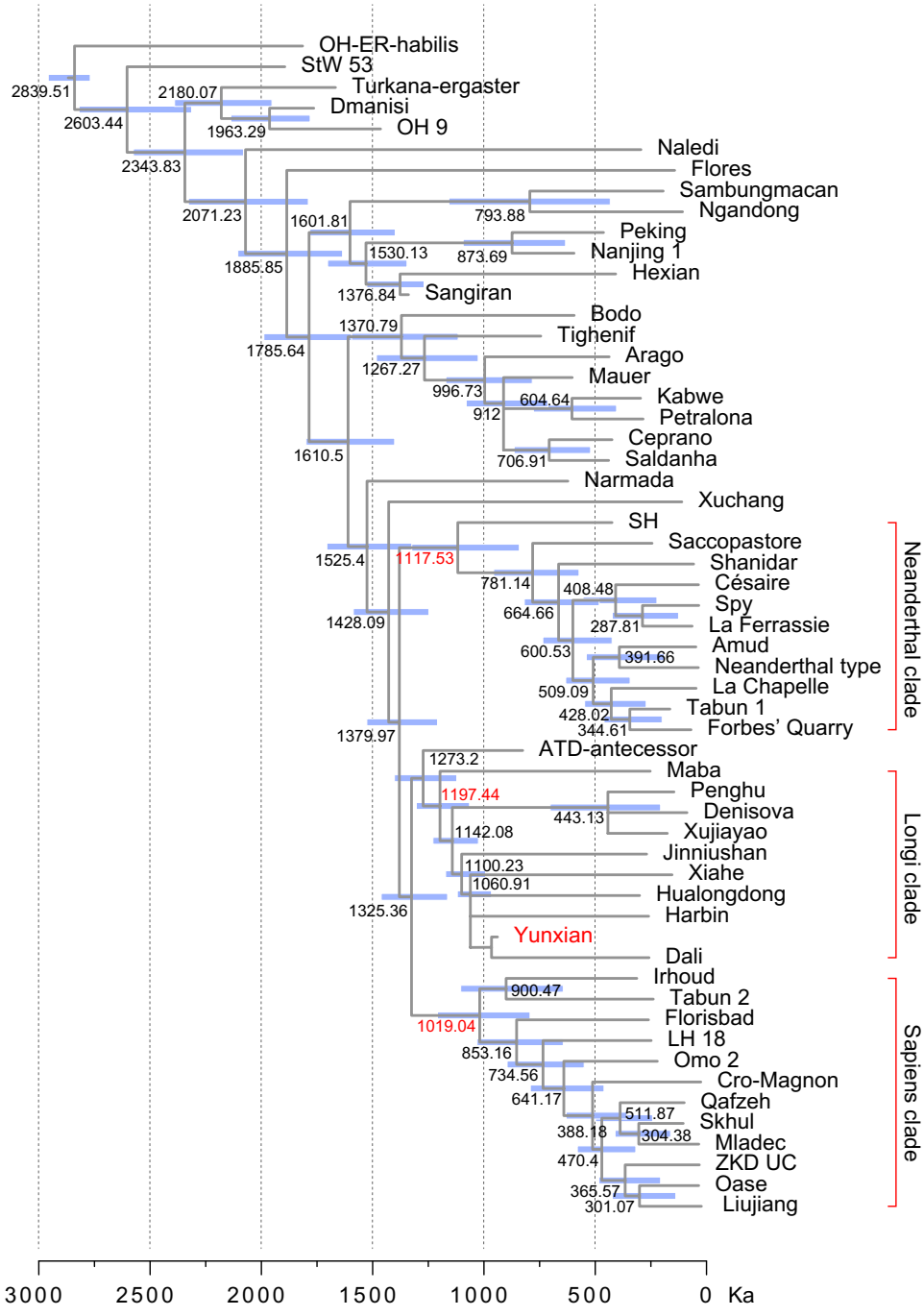


Fig. 4. Phylogeny and divergence time of the 57 selected fossil operational taxonomic units from the genus *Homo*. The topology of the tree was the majority consensus of the most parsimonious trees from the parsimony analysis in TNT (*34*). The divergence time was inferred from the Bayesian tip-dating analysis in MrBayes 3.2 (*35*). Branch lengths are proportional to the division age in thousands of years (Ka). Numbers at the internal nodes are the median ages, and the blue bars indicate the 95% highest posterior density interval of the node ages. The red half-brackets on the right indicate the ranges of the Neanderthal, longi, and sapiens clades. The numbers in red highlight the ages of division of the three clades. Yunxian is also highlighted in red.

Deep divergence

Previous estimates of the divergence time between Neanderthals and *H. sapiens* are about 0.5 to 0.7 Ma (*29*–*31*). However, recent evolutionary genetic studies based on a large number of modern and ancient genomes of *H. sapiens*, Neanderthals, and Denisovans have suggested a much deeper ancestry and population divergence in *H. sapiens* (*32*, *33*). Our Bayesian tip-dating analysis also revealed that the diversification of *Homo* and the origin of *H. sapiens* have much greater time depths (Fig. 4). The origin of the longi clade can be inferred to be about 1.2 Ma, slightly older than the Yunxian fossils. The origin of the sapiens clade is estimated to be about 1.02 Ma, also close to the age of Yunxian. The divergence between the longi clade and the sapiens clade is at about 1.32 Ma. The monophyletic Neanderthal clade, widely thought to be sister to *H. sapiens*, diverged from the longi and sapiens clades at about 1.38 Ma in our analysis.

Given its geological age of 0.94 to 1.10 Ma (*5*), Yunxian is close to the theoretical time of origin of the longi and sapiens clades. Phylogenetically, it is nested within the longi clade. However, its mosaic morphology, which retains plesiomorphies seen in *H. erectus*/*H. ergaster*, Kabwe, and

Downloaded from https://www.science.org at Tsinghua University on September 26, 2025

Petralona while developing apomorphies shared with *H. longi* and *H. sapiens*, may preserve transitional features close to the clade's origin. The narrow temporal gap between Yunxian and deeper longi nodes suggests rapid early diversification of the longi clade, as in the sapiens and Neanderthal clades.

REFERENCES AND NOTES

1. L. R. Berger *et al.*, *eLife* **4**, e09560 (2015).
2. M. W. Tocheri, *Nature* **568**, 176–178 (2019).
3. Q. Ji, W. Wu, Y. Ji, Q. Li, X. Ni, *Innovation (Camb.)* **2**, 100132 (2021).
4. T.-M. Chen, Q. Yang, Y.-Q. Hu, W.-B. Bao, T.-Y. Li, *Quat. Sci. Rev.* **16**, 455–458 (1997).
5. J.-J. Bahain *et al.*, *Anthropologie* **121**, 215–233 (2017).
6. T. Li, D. A. Etler, *Nature* **357**, 404–407 (1992).
7. H. de Lumley, *C. R. Séances Acad. Inscr. B.-Lett.* **153e année**, 119–123 (2009).
8. C. P. E. Zollikofer *et al.*, *Nature* **434**, 755–759 (2005).
9. G. Suwa *et al.*, *Science* **326**, 68e1–68e7 (2009).
10. S. Benazzi, F. L. Bookstein, D. S. Strait, G. W. Weber, *J. Hum. Evol.* **61**, 75–88 (2011).
11. S. Benazzi, G. Gruppioni, D. S. Strait, J.-J. Hublin, *Am. J. Phys. Anthropol.* **153**, 154–160 (2014).
12. F. Spoor *et al.*, *Nature* **519**, 83–86 (2015).
13. K. D. Pugh *et al.*, *Proc. Natl. Acad. Sci. U.S.A.* **120**, e2218778120 (2023).
14. F. Di Vincenzo *et al.*, *Sci. Rep.* **7**, 13974 (2017).
15. C. Buzi *et al.*, *Symmetry (Basel)* **13**, 1611 (2021).
16. D. Lewis, *Nature* **612**, 200–201 (2022).
17. A. Vialet *et al.*, *C. R. Palevol* **9**, 331–339 (2010).
18. E. M. Poza-Rey, A. Gómez-Robles, J. L. Arsuaga, *J. Hum. Evol.* **129**, 67–90 (2019).
19. X. Ni *et al.*, *Innovation (Camb.)* **2**, 100130 (2021).
20. C. J. Bae, X. Wu, *Nat. Commun.* **15**, 9479 (2024).
21. J. Krause *et al.*, *Nature* **464**, 894–897 (2010).
22. D. Reich *et al.*, *Nature* **468**, 1053–1060 (2010).
23. M. Meyer *et al.*, *Nature* **505**, 403–406 (2014).
24. V. Slon *et al.*, *Sci. Adv.* **3**, e1700186 (2017).
25. S. Sawyer *et al.*, *Proc. Natl. Acad. Sci. U.S.A.* **112**, 15696–15700 (2015).
26. M. Meyer *et al.*, *Science* **338**, 222–226 (2012).
27. E. A. Bennett *et al.*, *Sci. Adv.* **5**, eaaw3950 (2019).
28. Z. e. Lv, Ed., *The Jinniushan Hominin Site* (Cultural Relics Press, 2021).
29. A. Bergström, C. Stringer, M. Hajdinjak, E. M. L. Scerri, P. Skoglund, *Nature* **590**, 229–237 (2021).
30. L. Bokelmann *et al.*, *Proc. Natl. Acad. Sci. U.S.A.* **116**, 15610–15615 (2019).
31. M. Meyer *et al.*, *Nature* **531**, 504–507 (2016).
32. A. W. Wohns *et al.*, *Science* **375**, eabi8264 (2022).
33. T. Cousins, A. Scally, R. Durbin, *Nat. Genet.* **57**, 856–864 (2025).
34. P. A. Goloboff, J. S. Farris, K. C. Nixon, *Cladistics* **24**, 774–786 (2008).
35. F. Ronquist *et al.*, *Syst. Biol.* **61**, 539–542 (2012).

ACKNOWLEDGMENTS

We thank Y. Hou and N. Ma for help with CT scanning and surface modeling. W. Zhang helped with cluster computing. We thank C. Venditti, S. White, and T. Puschel for helpful discussions and reexamination of the Bayesian analysis. Images and CT scans of specimens from the National Museum of Kenya (NMK) are courtesy of NMK and The Human Fossil Record: A Digital Resource for Research and Education (https://human-fossil-record.org/). CT scans of Steinheim were provided by the State Museum of Natural History Stuttgart and the Department of Human Evolution, Max Planck Institute for Evolutionary Anthropology. We thank G. Manzi, C. Buzi, F. Di Vincenzo, A. Profico, and their team members for providing digital reconstructions of Steinheim and Ceprano. We thank the Anthropology staff at the Natural History Museum London (NHM) for provision of comparative material. This paper is a contribution to the NHM's Evolution of Life research theme. **Funding:** National Natural Science Foundation of China grant 42588201 (X.N.); National Key Research and Development Program of China grant 2023YFF0804502 (X.N., Q.L., C.Z.); Key Project of Beijing Social Science Foundation grant 22LSA022 (X.F.). The research of C.S. is supported by the Calleva Foundation (grant SDV17014) and the Human Origins Research Fund (grant SDV06001). **Author contributions:** Conceptualization: X.N., C.S.; Methodology: X.N., D.L., Q.Y., C.Z., C.S.; Investigation: X.F., D.L., Q.Y., F.G., Q.L., C.Z., C.S., X.N.; Visualization: D.L., Q.Y., X.N.; Funding acquisition: X.N.; Project administration: X.N.; Supervision: X.N.; Writing – original draft: X.N., C.S.; Writing – review & editing: X.N., C.S., X.F., D.L., F.G., Q.Y., Q.F., Y.F., X.H., C.T., H.Z., Q.L., C.Z. **Competing interests:** The authors declare that they have no competing interests. **Data and materials availability:** All data are available in the main text, the supplementary materials, and MorphoBank (Project 4045). The Yunxian 1 and Yunxian 2 crania are housed at the Hubei Museum, Hubei Province, China. The fossils can be accessed by sending a request to the Hubei Museum. **License information:** Copyright © 2025 the authors, some rights reserved; exclusive licensee American Association for the Advancement of Science. No claim to original US government works. https://www.science.org/about/science-licenses-journal-article-reuse

SUPPLEMENTARY MATERIALS

science.org/doi/10.1126/science.ado9202
Materials and Methods; Supplementary Text; Fig. S1 to S33; Tables S1 to S7; References (*36*–*145*); MDAR Reproducibility Checklist; Appendices 1 to 8

Submitted 28 February 2024; resubmitted 21 February 2025; accepted 30 July 2025
10.1126/science.ado9202

Downloaded from https://www.science.org at Tsinghua University on September 26, 2025